

Electrostatic Backscattering by Insulating Obstacles

M. Hanke^{a,*}, L. Warth^a

^a*Institut für Mathematik, Johannes Gutenberg-Universität Mainz, 55099 Mainz, Germany*

Abstract

We introduce and analyze backscatter data for a three dimensional obstacle problem in electrostatics. In particular, we investigate the asymptotic behavior of these data as, (i), the measurement point goes to infinity, and (ii), the obstacles shrink to individual points. We also provide numerical simulations of these data.

Keywords: electrostatics, obstacle problem, backscatter data

1. Introduction

Backscatter is a notion for the scattered field – which can be an acoustic or an electromagnetic wave – at the very same location where the incident field has been emitted. Its advantage is that a single sensor is sufficient to take these data. Moreover, for time harmonic excitations, these sensors can be designed in such a way that they only record the scattered field at the excitation point, and not the total field, cf., e.g., Griffiths [5]. Accordingly, backscatter can be measured much more accurately than the scattered wave at any other point, as the incoming field usually dominates the scattered field. It is therefore of practical interest to ask whether these data are sufficiently “rich” to solve the inverse problem of reconstructing the scatterer. Unfortunately, however, this problem is so far unsolved; we refer to [6, 10, 13, 14] for some partial results.

Nevertheless, inspired by this open problem, we have recently extended the notion of backscatter data to the two dimensional impedance tomography problem, where currents and voltages are measured at the boundary of a planar body. For this application complex variables techniques can be used to settle uniqueness for the inverse problem of reconstructing an insulating obstacle within the body from these “backscatter” data, cf. [8]; subsequently, in [7, 9, 11] constructive algorithms have been developed to approximate the obstacle from these data.

As a step towards the scattered wave problem we study in this note the analog of backscatter measurements for the Laplace equation in three dimen-

*Corresponding author

Email address: hanke@math.uni-mainz.de (M. Hanke)

sional free space, given the presence of insulating obstacles. With regard to the standard physical interpretation of the free space Laplace equation we call this electrostatic backscatter. If one wishes, however, this setting can alternatively be viewed as a simplistic low-frequency model for the backscatter of a time harmonic acoustic pressure wave, reflected from a sound-hard scatterer.

In Section 3 we provide some first qualitative properties of these data, that is, we show that they are positive and decay like $O(|x|^{-4})$ to zero, as the measurement point x goes to infinity. Then, in Section 4, we determine the asymptotic behavior of the backscatter at some fixed location, when the obstacles shrink to distinct points, similar to our findings from [7] for the backscatter in impedance tomography. We leave it for future work to utilize these results for the inverse problem.

Finally, we conclude this paper in Section 5 with numerical simulations taken from [15] to enhance further insight into the information content of the electrostatic backscatter of two insulating inclusions, and with a final summary.

2. Electrostatic backscatter

Let $\Omega \subset \mathbb{R}^3$ be a nonempty and bounded domain consisting of J connected C^2 -components Ω_j , $j = 1, \dots, J$, with connected complements $\mathbb{R}^3 \setminus \overline{\Omega}_j$. We denote the boundary of Ω by Γ , and those of Ω_j by Γ_j , respectively. We assume that the closures of Ω_j are mutually disjoint, and associate with them the support of electrically insulating obstacles. Inserting a unit charge at a point $x \in \mathbb{R}^3 \setminus \overline{\Omega}$, this gives rise to an electrostatic potential

$$U(y; x) = \Phi(y, x) + u(y; x), \quad y \in \mathbb{R}^3 \setminus \overline{\Omega}, \quad (1)$$

where

$$\Phi(y, x) = \frac{1}{4\pi} \frac{1}{|y - x|}, \quad y \neq x,$$

is the fundamental solution of the Laplacian, and $u(\cdot; x)$ is a harmonic function in $\mathbb{R}^3 \setminus \overline{\Omega}$ that satisfies the boundary condition

$$\frac{\partial}{\partial y \nu} u(y; x) = -\frac{\partial}{\partial y \nu} \Phi(y, x), \quad y \in \Gamma. \quad (2)$$

Here, ν is the exterior normal of Ω , and u is assumed to converge to zero as $|y| \rightarrow \infty$, uniformly for all directions. Such a solution $u(\cdot; x)$ of this exterior Neumann problem for the Laplacian is known to exist and is uniquely defined, cf., e.g., Kress [12]; it is the induced potential due to the insulator, given a point charge at x . We also mention that the potential U of (1) is nothing else than the Neumann function $N(y, x)$ for the Laplacian in the exterior of Ω .

If we assume that the potential $u(\cdot; x)$ is only known at the location of the point source, then the corresponding data

$$b(x) = u(x; x), \quad x \in \mathbb{R}^3 \setminus \overline{\Omega}, \quad (3)$$

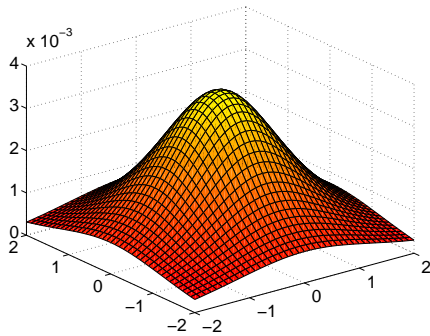


Figure 1: Backscatter data for the unit ball on an interval $\mathcal{M} = [-2, 2]^2 \times \{2\}$.

will be called the *electrostatic backscatter* of the obstacles Ω .

While in this paper we only investigate qualitative and quantitative properties of the backscatter, our ultimate interest is in the inverse problem: Given the backscatter $b|_{\mathcal{M}}$ on some two-dimensional manifold $\mathcal{M} \subset \mathbb{R}^3 \setminus \overline{\Omega}$, is it possible to determine Ω from these data – up to trivial symmetries? (For example, if \mathcal{M} is a hyperplane then the backscatter $b|_{\mathcal{M}}$ obviously cannot discern on which side of the plane a certain obstacle is located.)

Example 1. As a simple example we consider a single ball Ω for which the backscatter can be calculated analytically, due to the knowledge of the associated Neumann function. To be precise, if Ω is the unit ball of \mathbb{R}^3 , then

$$N(y, x) = \frac{1}{4\pi} \left(\frac{1}{|x - y|} + \frac{1}{|x| |x^* - y|} + \log \frac{|x||y| - x \cdot y}{1 - x \cdot y + |x| |x^* - y|} \right) \quad (4)$$

is the associated exterior Neumann function for $x, y \notin \overline{\Omega}$, and y not on the ray from the origin to infinity passing through x , cf., e.g., Barton [3]. Here, $x^* = x/|x|^2$ denotes the reflection of x at the unit sphere. For $y = \alpha x$ with $\alpha > 0$, $\alpha \neq 1$, and $|x|, |y| > 1$, (4) extends continuously to

$$N(\alpha x, x) = \frac{1}{4\pi} \left(\frac{1}{|\alpha - 1||x|} + \frac{1}{\alpha|x|^2 - 1} + \log \frac{\alpha|x|^2 - 1}{\alpha|x|^2} \right).$$

It thus follows that

$$b(x) = \lim_{y \rightarrow x} (N(y, x) - \Phi(y, x)) = \frac{1}{4\pi} \left(\frac{1}{|x|^2 - 1} - \log \frac{|x|^2}{|x|^2 - 1} \right) \quad (5)$$

for $|x| > 1$. Figure 1 shows the graph of the backscatter b over a horizontal axiparallel square \mathcal{M} that is centered two units above the origin, with sides that are four units long.

Using the inequality $\log(1 + t) < t$ for $t > 0$, it is easy to see that the backscatter (5) is positive throughout the exterior of the closed unit ball. Moreover, the backscatter only depends on the distance $|x|$ from the origin, and decays monotonically to zero with increasing distance. Accordingly, the electrostatic backscatter is largest right above the center of the ball. \square

3. General qualitative results

As we have seen in Example 1, the electrostatic backscatter of an insulating ball is strictly positive in the exterior of the closed ball. We show next that this property holds for any finite number of insulating obstacles.

Proposition 2. *Let Ω fulfill the assumptions in Section 2. Then the electrostatic backscatter associated with Ω is strictly positive in $\mathbb{R}^3 \setminus \overline{\Omega}$.*

PROOF. From Green's formula for the exterior of $\overline{\Omega}$, and from (2), it is easy to deduce that for every $x \in \mathbb{R}^3 \setminus \overline{\Omega}$ there holds

$$\begin{aligned} b(x) &= u(x; x) = \int_{\Gamma} \left(u(y; x) \frac{\partial}{\partial y\nu} \Phi(x, y) - \frac{\partial}{\partial y\nu} u(y; x) \Phi(x, y) \right) ds(y) \\ &= - \int_{\Gamma} u(y; x) \frac{\partial}{\partial y\nu} u(y; x) ds(y) + \int_{\Gamma} \frac{\partial}{\partial y\nu} \Phi(x, y) \Phi(x, y) ds(y) \\ &= \int_{\mathbb{R}^3 \setminus \overline{\Omega}} |\nabla_y u(y; x)|^2 dy + \int_{\Omega} |\nabla_y \Phi(x, y)|^2 dy, \end{aligned}$$

which is strictly positive. Note that we have used in the last equality that the gradient of a harmonic function that is bounded in the exterior of a bounded domain is also square integrable in the exterior of that domain ([12, p. 74]). \square

For the sequel we fix $x \in \mathbb{R}^3 \setminus \overline{\Omega}$, and define the potential

$$w(y) = \begin{cases} u(y; x), & y \in \mathbb{R}^3 \setminus \overline{\Omega}, \\ -\Phi(y, x), & y \in \Omega, \end{cases} \quad (6)$$

which is harmonic in $\mathbb{R}^3 \setminus \Gamma$, and decays at infinity. Moreover, by virtue of (2), w has a continuous flux across Γ . We can therefore rewrite w as a double layer potential over Γ with density

$$\psi(z) = [w]_{\Gamma}, \quad (7)$$

where $[w]_{\Gamma} = w_{\Gamma}^+ - w_{\Gamma}^-$ is the height of the jump (i.e., the exterior trace w_{Γ}^+ minus the interior trace w_{Γ}^- of w on Γ , cf., e.g., [12]):

$$w(y) = \int_{\Gamma} \psi(z) \frac{\partial}{\partial z\nu} \Phi(y, z) ds(z), \quad y \notin \Gamma. \quad (8)$$

We also define the associated double layer integral operator

$$(K\psi)(y) = \int_{\Gamma} \psi(z) \frac{\partial}{\partial z\nu} \Phi(y, z) ds(z), \quad y \in \Gamma, \quad (9)$$

over Γ , as well as the individual double layer integral operators

$$(K_j \psi_j)(y) = \int_{\Gamma_j} \psi_j(z) \frac{\partial}{\partial z\nu} \Phi(y, z) ds(z), \quad y \in \Gamma_j, \quad (10)$$

for $j = 1, \dots, J$. All these integral operators are well-defined as operators between the corresponding spaces of continuous functions.

Using the jump relations of double layer potentials, we obtain a second kind integral equation for ψ , namely

$$(I - 2K)\psi = \psi - \psi - 2w_\Gamma^- = 2\Phi(\cdot, x). \quad (11)$$

Recall that $I - 2K_j$ has a trivial null space, and hence, by the Riesz theory, is continuously invertible. The same argument (cf., e.g., the proof of Theorem 6.20 in [12]) can be used to show that $I - 2K$ is invertible. Accordingly, the density ψ is uniquely determined from (11). Summarizing our findings so far, we obtain from (3), (6), and (8) that

$$b(x) = w(x) = \int_\Gamma \psi(z) \frac{\partial}{\partial z\nu} \Phi(x, z) \, ds(z), \quad (12)$$

with ψ the unique solution of (11). We emphasize that x is still fixed in (12), and that the density ψ depends on the particular choice of x .

Before we can investigate the backscatter when x goes to infinity we also need to introduce the so-called polarization tensor (cf., e.g., Ammari and Kang [2])

$$M = 2 \int_\Gamma \nu(y) \left((I - 2K)^{-1} y^T \right) \, ds(y) \in \mathbb{R}^{3 \times 3} \quad (13)$$

associated with the insulating obstacles Ω .¹ We will utilize below that the polarization tensor of some obstacle(s) Ω is always symmetric and positive definite.

Theorem 3. *Let Ω fulfill the assumptions in Section 2. Then the electrostatic backscatter associated with Ω satisfies*

$$b(x) = \frac{1}{(4\pi)^2} \frac{x}{|x|^3} \cdot M \frac{x}{|x|^3} + O(|x|^{-5}), \quad |x| \rightarrow \infty,$$

uniformly for all directions. where the polarization tensor M is given by (13).

PROOF. We start with the observation that

$$\Phi(y, x) = \frac{1}{4\pi} \frac{1}{|x|} + \frac{1}{4\pi} \frac{x \cdot y}{|x|^3} + O(|x|^{-3}), \quad (14)$$

and

$$\frac{\partial}{\partial z\nu} \Phi(x, z) = \frac{1}{4\pi} \frac{\nu \cdot (x - z)}{|x - z|^3} = \frac{1}{4\pi} \frac{x \cdot \nu}{|x|^3} + O(|x|^{-3}), \quad (15)$$

¹In (13), ν and y are considered to be column vectors. Also note the slight abuse of notation: $(I - 2K)^{-1} y^T$ denotes the preimage $(I - 2K)^{-1} \text{id}$ of the identity function, $\text{id}(z^T) = z^T$ for every $z \in \Gamma$, evaluated at $y \in \Gamma$.

as z stays bounded and $|x|$ goes to infinity, uniformly for all directions. Next we recall that

$$\int_{\Gamma_j} \frac{\partial}{\partial z \nu} \Phi(y, z) \, ds(z) = \begin{cases} -1/2, & y \in \Gamma_j, \\ 0, & y \in \mathbb{R}^3 \setminus \overline{\Omega_j}, \end{cases} \quad (16)$$

and hence, densities ψ that are constant on every connected component of Γ are eigenfunctions of K . It thus follows from (14) that the solution ψ of (11) satisfies

$$\psi(y) = \frac{1}{4\pi} \frac{1}{|x|} + \frac{1}{2\pi} \frac{x}{|x|^3} \cdot (I - 2K)^{-1}y + O(|x|^{-3}), \quad (17)$$

uniformly on all of Γ and for all x sufficiently large. Using (16) once more we conclude that the constant part of ψ does not affect the value (12) of the backscatter, and hence, the assertion follows from inserting (15) and (17) into (12). \square

4. Small insulating obstacles

In the sequel we consider the situation when the obstacles are of the form

$$\Omega_j = z_j + \varepsilon O_j, \quad j = 1, \dots, J, \quad (18)$$

where z_j are distinct points in \mathbb{R}^3 , and O_j are bounded and connected C^2 -domains with connected complements $\mathbb{R}^3 \setminus O_j$. Moreover, we assume that $\varepsilon > 0$ is so small that the closures of Ω_j are mutually disjoint. We are interested in the asymptotic behavior of the backscatter as $\varepsilon \rightarrow 0$, in the spirit of, e.g., the results in [2]; we refrain, however, from adding subscripts ε to the backscatter b and the domains Ω_j , in order to keep the notation simple.

For the asymptotic analysis of the backscatter we require the following fundamental result.

Lemma 4. *Let K and K_j be the double layer integral operators in (9), resp. (10). Then $I - 2K$ is invertible, and its inverse is uniformly bounded as $\varepsilon \rightarrow 0$. Moreover, if $g \in C(\Gamma)$ and $\psi = (I - 2K)^{-1}g$, then*

$$\psi|_{\Gamma_j} = (I - 2K_j)^{-1}g|_{\Gamma_j} + r_j,$$

where the remainder satisfies

$$\|r_j\|_{\Gamma_j} \leq c\varepsilon^2 \|g\|_{\Gamma}, \quad (19)$$

$j = 1, \dots, J$, for some constant $c > 0$. Here, $\|\cdot\|_G$ refers to the maximum norm of $C(G)$ for a given compact set G .

PROOF. This result is known, essentially. Its proof can follow the arguments that are developed in detail in Sections 4, 5, and the appendix of [1]. \square

To derive the asymptotic form of the backscatter (12) we first expand

$$\Phi(y, x) = \Phi(x, y) = \Phi(x, z_j) + \nabla_z \Phi(x, z_j) \cdot (y - z_j) + O(\varepsilon^2)$$

for $y \in \Gamma_j$, and hence, rewrite (11) as

$$(I - 2K)\psi = g^{(0)} + g^{(1)} + h, \quad (20)$$

where $g^{(0)}$ is constant on each connected component of Γ ,

$$g^{(1)}(y) = 2 \nabla_z \Phi(x, z_j) \cdot (y - z_j) = O(\varepsilon), \quad y \in \Gamma_j, \quad (21)$$

and $\|h\|_\Gamma = O(\varepsilon^2)$, uniformly on all of Γ , and for all x with distance $d(x, \Omega) \geq \delta$ for any chosen $\delta > 0$.

Using the same argument as in the proof of Theorem 3 we conclude from (16) that

$$b(x) = \int_\Gamma \psi^{(1)}(z) \frac{\partial}{\partial z \nu} \Phi(x, z) \, ds(z) + O(\varepsilon^4) \quad (22)$$

with

$$\psi^{(1)} = (I - 2K)^{-1} g^{(1)} = O(\varepsilon), \quad (23)$$

where, in (22), we have taken into account that $(I - 2K)^{-1}$ is uniformly bounded according to Lemma 4, and that the remainder h in (20), and the surface measure $|\Gamma|$ of Γ , are both $O(\varepsilon^2)$.

Employing another Taylor expansion, we obtain

$$\frac{\partial}{\partial z \nu} \Phi(x, z) = \nu(z) \cdot \nabla_z \Phi(x, z_j) + O(\varepsilon), \quad (24)$$

uniformly for $z \in \Gamma_j$, $j = 1, \dots, J$, and $d(x, \Omega) \geq \delta$, and inserting this into (22), we conclude that

$$b(x) = \sum_{j=1}^J \nabla_z \Phi(x, z_j) \cdot \int_{\Gamma_j} \psi^{(1)}(z) \nu(z) \, ds(z) + O(\varepsilon^4), \quad (25)$$

where, again, we have used that $|\Gamma_j| = O(\varepsilon^2)$, and estimated $\psi^{(1)}$ as in (23).

Finally, it remains to derive from (23) the asymptotic form of $\psi^{(1)}$ by means of Lemma 4, which states that

$$\psi^{(1)}|_{\Gamma_j} = (I - 2K_j)^{-1} g^{(1)}|_{\Gamma_j} + r_j, \quad j = 1, \dots, J, \quad (26)$$

with, cf. (21),

$$\|r_j\|_{\Gamma_j} \leq c\varepsilon^2 \|g^{(1)}\|_\Gamma = O(\varepsilon^3),$$

the constant being independent of $j = 1, \dots, J$. Inserting the definition (21) of $g^{(1)}$ we thus obtain that

$$\psi^{(1)}|_{\Gamma_j} = 2 \left((I - 2K_j)^{-1} (\cdot - z_j) \right) \cdot \nabla_z \Phi(x, z_j) + O(\varepsilon^3).$$

Transforming the integrals (25) and (10) to integrals over ∂O_j via the substitution $\eta = (z - z_j)/\varepsilon$, $z \in \Gamma_j$, we eventually arrive at (cf. [1], again, for a similar computation)

$$b(x) = \varepsilon^3 \sum_{j=1}^J \nabla_z \Phi(x, z_j) \cdot M_j \nabla_z \Phi(x, z_j) + O(\varepsilon^4), \quad (27)$$

where the matrices

$$M_j = 2 \int_{\partial O_j} \nu(\eta) \left((I - 2\widehat{K}_j)^{-1} \eta^T \right) ds(\eta) \in \mathbb{R}^{3 \times 3}, \quad (28)$$

$j = 1, \dots, J$, are the polarization tensors associated with the insulating domains O_j , and

$$(\widehat{K}_j \chi)(\eta) = \int_{\partial O_j} \chi(\zeta) \frac{\partial}{\partial \zeta \nu} \Phi(\eta, \zeta) ds(\zeta), \quad \eta \in \partial O_j,$$

denotes the double layer integral operator over ∂O_j .

We summarize our findings in the following theorem.

Theorem 5. *The electrostatic backscatter corresponding to the insulating domains $\Omega = \bigcup \Omega_j$ of (18) has the asymptotic form*

$$b(x) = \varepsilon^3 \sum_{j=1}^J \nabla_z \Phi(x, z_j) \cdot M_j \nabla_z \Phi(x, z_j) + O(\varepsilon^4), \quad \varepsilon \rightarrow 0,$$

with the polarization tensors $M_j \in \mathbb{R}^{3 \times 3}$ defined in (28); the remainder estimate is uniform for all $x \in \mathbb{R}^3$ with $d(x, \Omega) \geq \delta$ for any $\delta > 0$.

Example 6. For O_j the unit disk, the polarization tensor is the three by three identity matrix, multiplied by 2π , cf. [2, Chapter 4], and the associated term of the backscatter in (27) behaves like

$$\frac{1}{8\pi} \varepsilon^3 |x - z_j|^{-4}, \quad \varepsilon \rightarrow 0.$$

In fact, if Ω is a ball of radius ε , centered around the origin, then the corresponding exterior Neumann function is given by $\frac{1}{\varepsilon} N(y/\varepsilon, x/\varepsilon)$, with N of (4), and hence, the associated backscatter equals

$$\begin{aligned} b(x) &= \frac{1}{4\pi\varepsilon} \left(\frac{\varepsilon^2}{|x|^2 - \varepsilon^2} - \log \frac{|x|^2}{|x|^2 - \varepsilon^2} \right) = \frac{1}{4\pi\varepsilon} \left(\frac{1}{2} \frac{\varepsilon^4}{(|x|^2 - \varepsilon^2)^2} + O(\varepsilon^6) \right) \\ &= \frac{1}{8\pi} \frac{\varepsilon^3}{|x|^4} + O(\varepsilon^5) \end{aligned}$$

as $\varepsilon \rightarrow 0$. □

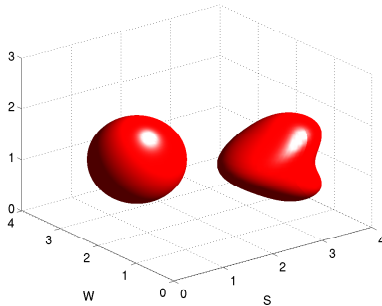


Figure 2: Two insulating objects in free space: a sphere and a heart.

Corollary 7. *The electrostatic backscatter corresponding to the insulating domains $\Omega = \bigcup \Omega_j$ of (18) satisfies*

$$b(x) \sim \varepsilon^3 \sum_{j=1}^J |x - z_j|^{-4},$$

where the \sim sign refers to the fact that the ratio of the expressions on its two sides is uniformly bounded from above and below by positive constants as $\varepsilon \rightarrow 0$, uniformly for x from any compact subset of $\mathbb{R}^3 \setminus \overline{\Omega}$.

PROOF. The result follows immediately from the fact that the polarization tensors M_j of (28) are positive definite matrices. \square

In other words, for small obstacles, the peaks of the backscatter along some hyperplane \mathcal{M} are asymptotically at the orthogonal projections of the locations of the obstacles; the height of these peaks can be used to approximately determine the distance of the obstacles.

5. A numerical example

While Theorem 5 and Corollary 7 are useful to get a rough idea of the qualitative form of the backscatter, we now report on numerical simulations in [15] for multiple obstacles of finite size to provide additional qualitative insight into these data. In these simulations the backscatter has been evaluated by solving the Neumann boundary value problems (2) for several measurement points x on some finite grid \mathcal{M}_Δ .

Figure 2 shows a particular setting with two insulating objects, a sphere and a heart shaped obstacle. The sphere has a radius $\rho = 0.8$, and its center has the coordinates $x = (x_1, x_2, x_3) = (1, \frac{34}{15}, \frac{4}{3})$; the heart is of comparable size, and its center of mass is approximately at $(2.9, 1.3, 1.1)$. For this example the backscatter has been computed on all six faces of the box $[0, 4]^2 \times [0, 3]$ that encloses both obstacles (the same box that is displayed in Figure 2). Backscatter

data have been generated via the solution of a boundary integral equation, using a standard single layer potential representation for u of (2), cf. [12].

The resulting second kind double layer integral equation has been solved with a spectral collocation method due to Ganesh, Graham, and Sivaloganathan [4]. This method is based on coordinate transformations that map the individual boundaries Γ_j to spheres, and hence, requires the obstacles to be equivalent to spheres, topologically. Then, for each sphere, the unknown densities are expanded in $2N \times (N - 1) + 2$ trigonometric ansatz functions in spherical coordinates (here, $N = 15$), and a corresponding number of collocation points on an equidistant spherical grid is used to set up the linear system. For each of these points, however, the sphere is rotated prior to the discretization of the integral in order to cancel the singularity of the double layer operator kernel with the singularity of the spherical coordinate transformation at the north pole.

Once the potential densities have been determined, the single layer potential is evaluated on equispaced grids on each of the six faces, with a spacing of $h = 0.1$ between neighboring points along every coordinate direction. The associated integrals are discretized with the same technique as before. Figure 3 displays the values of the backscatter: top and bottom plot show the backscatter at the top ($x_3 = 3$) and bottom ($x_3 = 0$) of the box, respectively; the four plots in the center correspond to the backscatter at the four vertical faces to the North ($x_2 = 4$), East ($x_1 = 4$), West ($x_1 = 0$), and South ($x_2 = 0$) of the box (compare Figure 2).

Due to the strong decay of the backscatter (see Theorem 3), its values at the four vertical faces depict only one of the obstacles each, essentially. The magnitude of the backscatter is connected to the distance between the respective face and the obstacles. The Eastern/Western faces of the box, being closer to the obstacles than the other two, exhibit significantly larger values of the backscatter. The Northern face is farthest away; its distance to the sphere is $d_N \approx 0.93$, whereas the distance between the heart and the Southern end of the box is $d_S \approx 0.54$. Taking the result of Theorem 3 into account, one would expect that the corresponding backscatter is about $(d_N/d_S)^{-4} \approx 0.11$ smaller at the Northern face than in the South. In fact, the maximal values are 0.0032 in the North, and 0.0124 in the South, which corresponds to a ratio of 0.26, roughly, and which is only by about a factor of two off from what has been expected.

Qualitatively, we observe that the Eastern and the bottom faces exhibit two local extrema: in the East this is due to the two “wings” of the heart; at the bottom the two extrema are caused by the two different objects. In contrast to that the backscatter at the top face (from which both objects are clearly “visible”) has only one maximal value corresponding to the (slightly closer) sphere; the longer tail of the data is the only indicator for the presence of a second object. A similar effect occurs when the heart is (slightly) moved towards the West: then the two peaks at the Eastern face smear out to one single peak.

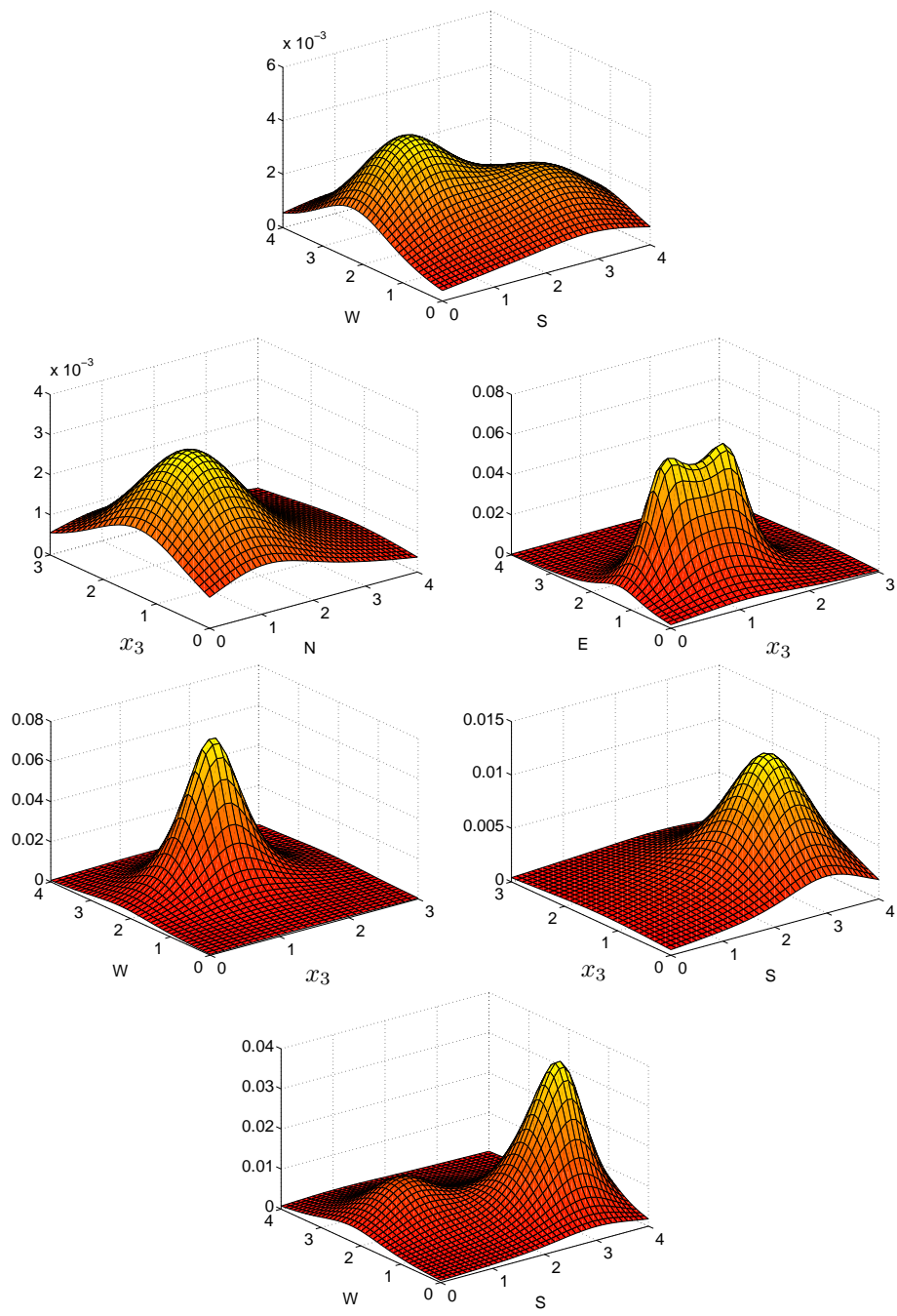


Figure 3: Backscatter for the two obstacles in Figure 2. See explanation in the text.

6. Summary

We have introduced a notion of electrostatic backscatter for insulating obstacles, in analogy to what is known as the backscatter of sound-hard scatterers in acoustics. As we have seen both theoretically and numerically, the electrostatic backscatter drops down to (almost) zero very quickly when moving away from the obstacles. We have also determined its approximate shape for small obstacles.

Concerning the corresponding inverse problem we can deduce that very close near-field data will necessarily be required to detect non-convex features of the obstacles. Even the number of the obstacles will be hard to determine from far-field data.

Acknowledgements

The authors are indebted to Prof. Michael Pidcock for pointing their attention to Barton's book [3] concerning the exterior Neumann function for the unit ball.

References

- [1] H. Ammari, R. Griesmaier, M. Hanke, Identification of small inhomogeneities: Asymptotic factorization, *Math. Comp.* 76 (2007) 1425–1448.
- [2] H. Ammari, H. Kang, *Polarization and Moment Tensors with Applications to Inverse Problems and Effective Medium Theory*, Springer, Ney York, 2007.
- [3] G. Barton, *Elements of Green's Functions and Propagation: Potentials, Diffusion, and Waves*, Clarendon Press, Oxford, 1989.
- [4] M. Ganesh, I. Graham, J. Sivaloganathan, A new spectral boundary integral collocation method for three-dimensional potential problems, *SIAM J. Numer. Anal.* 35 (1998) 778–805.
- [5] H. Griffiths, Magnetic induction tomography, in: D.S. Holder (Ed.), *Electrical Impedance Tomography*, Institute of Physics Publishing, Bristol, 2005, pp. 213–238.
- [6] H. Haddar, S. Kusiak, J. Sylvester, The convex back-scattering support, *SIAM J. Appl. Math.* 66 (2005) 591–615.
- [7] M. Hanke, Locating several small inclusions in impedance tomography from backscatter data, submitted, 2010.
- [8] M. Hanke, N. Hyvönen, S. Reusswig, An inverse backscatter problem for electric impedance tomography, *SIAM J. Math. Anal.* 41 (2009) 1948–1966.

- [9] M. Hanke, N. Hyvönen, S. Reusswig, Convex backscattering support in electric impedance tomography, *Numer. Math.* 117 (2011) 373–396.
- [10] P. Hähner, R. Kress, Uniqueness for a linearized, inverse obstacle problem using backscattering data, in: A. Bermúdez et al (Eds.), *Proceedings of the Fifth International Conference on Mathematical and Numerical Aspects of Wave Propagation*, SIAM, Philadelphia, 2000, pp. 489–493.
- [11] S. Hollborn, Reconstructions from backscatter data in electric impedance tomography, to appear in *Inverse Problems*, 2011.
- [12] R. Kress, *Linear Integral Equations*, 2nd edition, Springer, Berlin, 1999.
- [13] P. Ola, L. Päivärinta, and V. Serov, Recovering singularities from backscattering in two dimensions, *Comm. Partial Differential Equations* 26 (2001) 697–715.
- [14] J.M. Reyes, Inverse backscattering for the Schrödinger equation in 2D, *Inverse Problems* 23 (2007) 625–643.
- [15] L. Warth, *Elektrostatistische Rückstreuung im \mathbb{R}^3* , diploma thesis, Johannes Gutenberg-Universität, Mainz, Germany, 2010. In German.